ELSEVIER

Contents lists available at ScienceDirect

Chemical Physics Impact

journal homepage: www.sciencedirect.com/journal/chemical-physics-impact



Full Length Article

Enhancement of electrical and radiation shielding properties of vanadium doped lithium telluro-borate (LTB) glasses

S Karthika^a, S Shanmuga Sundari^b, K Marimuthu^c, P Meena^{a,*}

- ^a Department of Physics, PSGR Krishnammal College for Women, Coimbatore 641004, India
- ^b PG & Research Department of Physics, Seethalakshmi Ramaswami College, (Affiliated to Bharathidasan University) Trichy, 620002, India
- ^c Department of Physics, Gandhigram Rural Institute-Deemed to be University, Gandhigram 624302, India

ARTICLE INFO

Keywords:

Lithium telluro-borate glasses Tellurite glasses Vanadium doped glasses Enhanced electrical conductivity Radiation shielding glasses

ABSTRACT

Vanadium doped lithium telluro-borate (LTB) glasses of the composition $(20\text{-}x)\text{Li}_2\text{O}\text{-}20\text{TeO}_2\text{-}60\text{B}_2\text{O}_3\text{-}(x)\text{V}_2\text{O}_5$ (x=0,0.5,1,1.5 and 2 in mol %) were synthesised by melt quenching technique. The structural, optical, physical, electrical and radiation shielding parameters of the prepared glasses were investigated to determine the effect of vanadium in the LTB glass matrix. Density of LTB glasses were found to increases from 2.52 to 2.98 g/cm³ under addition of vanadium oxide and certain density derived structural parameters were studied. XRD pattern confirms the amorphous nature of the pristine and doped LTB glass. FTIR spectra shows the presence of various bonds in the vanadium doped LTB glasses. The direct optical bandgap (Eg) decreases due to the addition of V₂O₅ and leads to creation of defects in the LTB glasses thereby increasing the Urbach energy (Eu). Physical parameters like refractive index (n), molar refractivity (Rm), reflection loss (Lr), molar electronic polarizability (α_m), transmission coefficient (T) and metallization criteria (M) were calculated. The electrical properties including dielectric constant (ϵ '), conductivity (σ) and activation energies (Ea) were analysed and observed that Ea decreases under the addition of vanadium to the glass network proving the enhancement in electrical conductivity. Radiation shielding parameters such as MAC, LAC, HVL, TVL, MFP, R, ACS, ECS, N_{eff}, Z_{eff}, and C_{eff} were calculated using Phy-X/PSD and LTB_2V with the highest V₂O₅ additive shows enhanced result in gamma radiation shielding.

Introduction

Natural sources of radiation such as cosmic rays, terrestrial radiation, and man-made radioactive sources, like nuclear reactors are the major reason in the emission of alpha, gamma and X-rays. Radiation effects are harmful to the environment, therefore various researchers are working on radiation shielding and protective materials [1–3]. Materials that possess high density, refractive index and high atomic number were considered suitable for such application such as nuclear shielding, gamma ray telescopes and dosimeter application. Alloys, ceramics, polymers and concretes were used in general but since these materials were opaque and had limited applications. As an efficient alternative glass based radiation shielding materials came into utilization [4–6]. Glasses possess random network of structure with short range order, good transparency, hardness, and easy to manufacture. Glasses possess a unique property to accommodate foreign atoms in their interstitials. Glass formers therefore readily accept modifiers such as alkali,

transition metal and rare earth ions to loosen the glass network. The choice of host material and concentration plays an important role in the properties of glass.

When oxide-based glasses are considered, boron-based glasses (B₂O₃) have excellent glass forming properties like high transparency, low crystallization, low melting point, good thermal stability, and good dielectric constant [7,8]. Borates are good thermal conductors therefore have high phonon energy (1300–1500 cm⁻¹) which is used in applications like heat detectors and thermal insulating materials, it also resists vibrations, possess lower viscosity, lower cation, low refractive index, high conductivity, short range order and higher bond strength [9–12]. Borate possess BO₃ and BO₄ structural units and which under the addition of other formers /modifiers gives rise to non-bridging oxygens (NBOs). To decreases the hygroscopic nature of borates and to improve the glass transparency and refractive index tellurium is incorporated in the glass matrix. Tellurium increases the density of glass thereby increasing its refractive index. The addition of tellurium in the borate

E-mail address: drpmeena@gmail.com (P. Meena).

 $^{^{\}ast}$ Corresponding author.

glasses gives rise to mixed glass former effect (MGFE) leading to telluro-borate glasses [13]. TeO_2 also reduces the phonon energy thereby increasing the luminescence property of the borate-based glasses. TeO_2 are conditional glass formers that possess low melting point, good thermal and chemical stability. In addition, it has high non-linear refractive index and exhibits good nuclear shielding behaviour therefore used in gamma ray attenuators [11,12]. In addition to the above, tellurite based glasses exhibit good non-linear optical response [14]. To further reduce the melting temperature and to increase its thermal stability, network modifiers are added to telluro borate glasses. Alkali oxides such as Li_2O , Na_2O and K_2O when added to borate glasses lowers its viscosity and aid in formation of glasses. Alkali like lithium interacts with the glass matrix as ionic conductors and helps to shift the optical absorption edge to longer wavelengths.

Transition metal ions when added as glass modifiers, they alter the geometrical arrangement of the nearby glass forming network and impart their characteristic colours into the parent glass [15]. When an alkali (in this case Li) and/or transition metal ion (here V) based glass modifiers are added to the telluro-borate glasses there is an increase in NBO's due to changes in the BO₃, BO₄, TeO₃ to TeO₄ units. Mixing of vanadium in the lithium telluro-borate glasses improves luminescence property and increases its electrical conductivity. The exchange of electrons (hopping) between V⁴⁺ and V⁵⁺ states induce polarization around vanadium ions leading to formation of polarons [13]. These vanadium ions dissolve easily into the glass network and creates number of vacancies/ defects such as colour centres [16]. The formation of these colour centre helps in applications including optical signal processing, laser fabrication and memory devices. The vanadium content in the lithium telluro-borate glasses are not exceeded 2% in order to maintain sufficient transparency when glasses are used for luminescent converters [17]. The addition of transition metal like vanadium to the glass matrix is due to its peculiar property of very high thermal and electrical conductivity and high resistance to oxidation and corrosion. Some distinct application of vanadium doped borate glasses are in luminescence, high absorption and conductivity, nuclear waste management and change in activation energy of glasses. The influence of V2O5 in the structural, optical, electrical properties in borate glass systems are reported in recent times where the increase in NBOs results in major structural variation, the optical data shows good luminescence characteristics and decrease in bandgap. The electrical conductivity enhancement of various oxide glass systems due to this transition metal ion has been discussed by several researchers [16,18,19]. Rajinder Kaur et. al. has discussed the structural and thermal properties of vanadium tellurite glasses of the composition $x V_2 O_5 - (100 - x) \text{ TeO}_2$ (where x = 10, 30, 40,50 mol %) were the densities of the glasses decreases from 5.22 to 3.99 g/cm³. The XRD and Raman spectra were used to elucidate the short-range structure of vanadium tellurite glasses [20]. Lead free radiation shielding materials are the need of the hours where materials like bismuth, barium and tellurium are given importance. The radiation shielding behaviour of tellurium-based glasses has been an interesting topic and is studied intensely, some are 20TeO_2 -(30- x) B_2O_3 -30BaO-20Bi₂O₃- x Er_2O_3 glass systems, (70-BO-5TeO-20SrO-5ZnO- x BiO (with 0 \leq x \leq 15 mol %) system and bismuth titanium vanadium sodium tellurite glass system where the density of the specially-developed glass samples was increased from 2.21 to 4.01 g/cm 3 with the addition of Bi₂O₃ [21,22]. Several telluro-borate glass systems with addition of different transition metal ions and rare earth ions are have been reported as excellent shielding materials [23-27]. The novelty of the current work is based on effect of vanadium in lithium telluroborate glasses to enhance the electrical conductivity and to analyse the radiation shielding which is not reported elsewhere. Previous reports on vanadium-based tellurite glasses shows the enhanced electrical conductivity at room temperature and at higher temperatures due to V^{4+} ion content in the glass structure [28,29]. Therefore, vanadium based telluro-borate glasses were choosen for analysing the electrical conductivity and shielding ability.

In the present work, efforts are made to study the synthesis of lithium telluroborate glasses and the effect of vanadium (0,0.5,1,1.5 and 2 mol %) in the glasses for appropriate gamma ray shielding and enhanced electrical conductivity. The structural properties were studied using XRD, FTIR, RAMAN spectra, optical properties were discussed from UV-Vis spectrum. The dielectric constant and electrical conductivity were measured from room temperature to 575 K. The radiation shielding properties of the glasses against gamma radiation are also investigated using Phy-X/PSD.

Methods and materials

Experimental procedure

Lithium telluroborate (LTB) and vanadium doped LTB glasses of the composition $(20\text{-}x)\text{Li}_2\text{O} + 20\text{TeO}_2 + 60\text{B}_2\text{O}_3 + (x)\text{V}_2\text{O}_5$ (x=0,0.5,1,1.5 and 2 in mol %) were synthesized by melt quenching technique and the glass code and composition is listed in Table 1. Precursors of high purity 99.99 % were stoichiometrically weighed and grinded in agate motor and calcinated at 500 °C for 4 h. This calcinated froth was again grinded and melted at 900 °C for 2 h. The crucible was stirred periodically to get homogenous melt. The molten flux was quenched on a preheated stainless-steel mould and the glasses were annealed at 300 °C for 6 h to increase the mechanical stability, reduce thermal stress and strain. The glasses were allowed to cool to room temperature and then polished on both sides to get uniform thickness of 1.5 mm. Fig. 1 shows the prepared LTB, LTB_0.5V, LTB_1V, LTB_1.5V and LTB_2V based on V₂O₅ concentration of 0, 0.5, 1, 1.5 and 2 (mol %) respectively.

Characterization techniques

The densities of the glasses were measured by Archimedes principal using AUY220 Analytical Balance from Shimadzu with toluene as immersing liquid, XRD measurement was performed by Empyrean, Malvern PANalytical X-ray diffractometer using Cu- K_{α} with scan speed of 5°/min, step width 0.02° from 5° to 90°. FTIR spectral measurement was measured using IRAffinity-1S - compact Fourier transform infrared spectrophotometer in ATR mode. The Raman spectra was investigated by Laser confocal Raman microscope -Renishaw, UK (laser excitation wavelength of 785 nm) at 0.5 mW power with 30s acquisition time held at room temperature. The optical properties of the samples were analysed using Shimadzu UV-Visible spectrometer with 0.1 nm resolution for measuring 200-800 nm. The electrical properties like dielectric constant and A.C. conduction mechanism for the glasses was recorded from room temperature to 575 K at frequency ranging from 100 kHz to 2 MHz using Wayne Kerr ZM278 LCR meter. The radiation shielding parameters were determined using Phy-X/PSD software.

Table 1The composition of the prepared LTB and vanadium doped LTB glasses.

Glass codes	Composition of the prepared glasses (mol%)				
	B_2O_3	Li ₂ O	TeO ₂	V_2O_5	
LTB	60	20	20	0	
LTB_0.5V	60	19.5	20	0.5	
LTB_1V	60	19	20	1	
LTB_1.5V	60	18.5	20	1.5	
LTB_2V	60	18	20	2	



Fig. 1. Physical appearance of as-prepared LTB and vanadium doped LTB glasses.

Results and discussion

Structural properties

Density (ρ), Molar volume (V_m), Molar volume of oxygen (V_o), Oxygen packing density (OPD), Boron-boron separation (d_{B-B}) and bond density (n_b)

Density ρ is an important intrinsic property that provides information on short range order of the glass matrix. It is used to measure the degree of structural compactness, change in configuration and coordination number of the glass matrix. ρ was estimated from measuring the weight of glass in air and in immersing liquid of known density (toluene, $\rho=0.866~g/cm^3)$ from which density of the glasses were found using Archimedes' principle. The density of pristine LTB was $2.52~g/cm^3$ which increases under the addition of V_2O_5 to a maximum of $2.98~g/cm^3$ due to formation of non-bridging oxygen (NBO) this is in agreement with the report of Dalal et al. on vanadium doped zinc lithium borate glasses [30]. The addition of vanadium in the glass matrix has led to a compact structure with increase in network rigidity. As density increases V_m and V_o are found to decreases with increase in OPD as shown in Fig. 2 (a) and (b). The obtained values of V_m and V_o (in Table 2.) are decreasing from

 Table 2

 Structural parameters of the synthesized LTB and vanadium doped LTB glasses.

Structural parameters	LTB	LTB_0.5V	LTB_1V	LTB_1.5V	LTB_2V
Density ρ (g/cm ³)	2.52	2.54	2.55	2.77	2.98
Average molecular weight <i>AMW</i> (g)	79.67	79.78	79.89	80.00	80.11
Molar volume V_m (cm ³ /mol)	31.61	31.41	31.30	28.80	26.88
Molar volume of oxygen V_o (cm ³ /mol)	14.94	14.80	14.73	13.55	12.58
Oxygen packing density OPD (mol/cm ³)	66.93	67.52	67.85	73.78	79.45
Boron-Boron separation $d_{B-B} \ (\times \ 10^{-10} \ \mathrm{m}^2)$	8.17	8.15	8.15	7.92	7.75
Bond density n_b (× 10^{30} m ⁻³)	3.78	3.77	3.78	3.50	3.27
Optical basicity Λ_{th}	0.581	0.582	0.583	0.584	0.585
Ionicity I_c (%)	88.429	88.428	88.426	88.424	88.423
Covalent C_c (%)	11.570	11.571	11.573	11.575	11.576
Poisons ratio μ_{cal}	0.4686	0.4689	0.4690	0.4670	0.4691

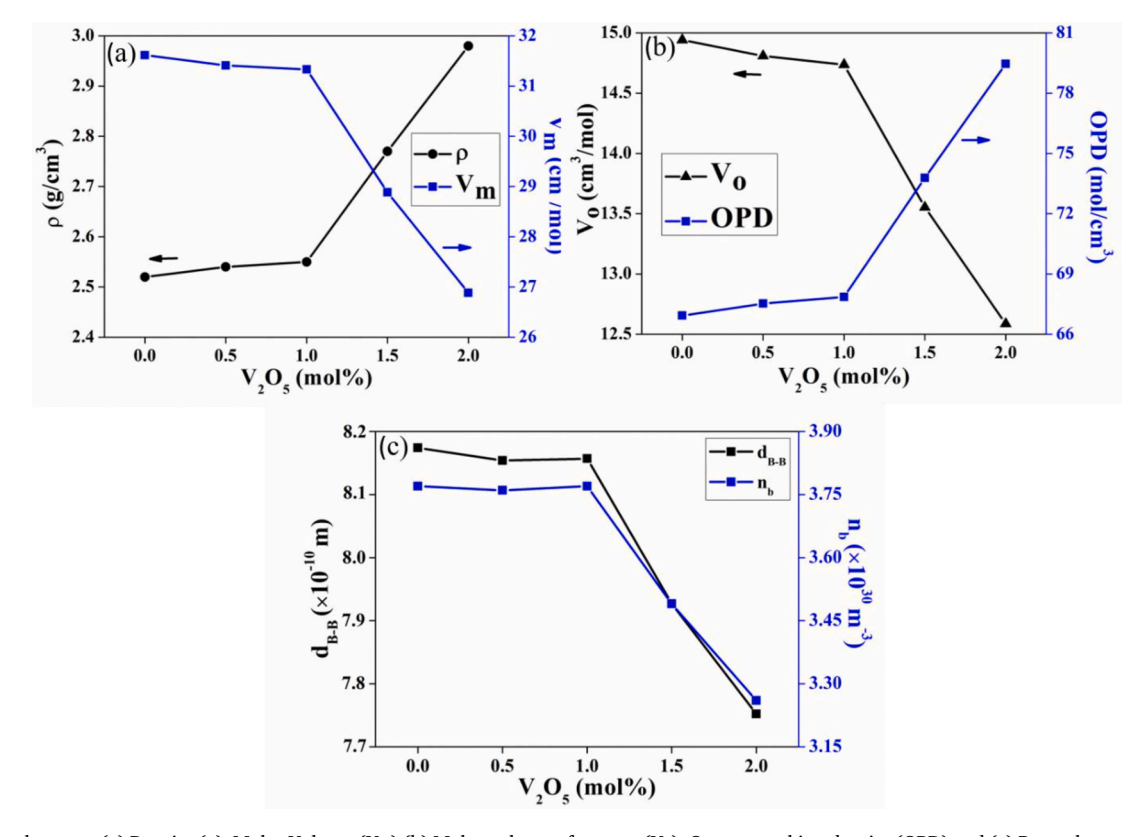


Fig. 2. Relation between (a) Density (ρ), Molar Volume (V_m) (b) Molar volume of oxygen (V_o), Oxygen packing density (OPD) and (c) Boron-boron separation (d_{B-B}) and bond density (n_b) of LTB and vanadium doped LTB glasses.

 $31.61~\rm cm^3/mol$ to $26.88~\rm cm^3/mol$ and $14.94~\rm cm^3/mol$ to $12.58~\rm cm^3/mol$ for LTB and LTB_2V glasses. The Boron-boron separation, $d_{B\text{-}B}$ (distance between two boron atoms) and bond density, n_b (distance between boron and oxygen) is found to decrease with addition of V_2O_5 and is shown in Fig. 2. (c). This may be due to increase in vanadium and oxygen, tellurium and oxygen bonds in the glass system and is discussed later in FTIR.

Optical basicity (Λ_{th}) , Ionicity (I_c) , Covalent (C_c) and Poisons ratio (μ_{cal}) .

The theoretical optical basicity Λ_{th} value was calculated for multi component glass system based on theory proposed by Yang et. al [31]. It was calculated depending on the algebraic sum of individual components in the glass matrix. Λ_{th} values for the prepared glasses were in the range 0.581 to 0.585 (refer Table 2). This is in good agreement with already reported vanadium based lithium glasses [30]. The increase in Λ_{th} reduces the covalent nature of oxygens in vanadium doped LTB glasses resulting in enhancement of sigma bond in the glasses. It also increases the bond lengths of vanadium and oxygen and in turn decrease in $d_{R,R}$ and n_h in addition of vanadium.

The synthesized LTB and vanadium doped LTB glasses possess about 88.43 % of ionic nature and 11.57 % of covalent nature and is shown in Table 2. This was estimated using electronegativity of anion and cations present in the glass matrix [32]. The influence of vanadium has led to decrease in ionic nature and increased the covalent nature of the LTB glasses. Poisons ratio μ_{cal} was calculated (to determine the rigidity of the glasses) from the packing density as mentioned in the earlier reports [33]. From Table 2 the μ_{cal} of all the prepared LTB and vanadium doped LTB glasses are about 0.46 denoting the low cross link density. The low cross link density indicates that the prepared glasses have good transmission and reduced scattering which makes it suitable for optical fibres application.

X-ray diffraction (XRD)

XRD is used to determine the crystalline nature of the sample. XRD pattern of prepared pristine LTB is shown in Fig. 3. The LTB glasses are found to be amorphous with short range order. There is a broad hump over the range $2\theta = 5^{\circ} - 30^{\circ}$ that indicate the disorder nature of the LTB glasses. The observed broad hump with no definite peaks confirms the non-crystalline nature of the pristine LTB glass. It also represents the random and chaotic arrangement of molecules in the glass matrix.

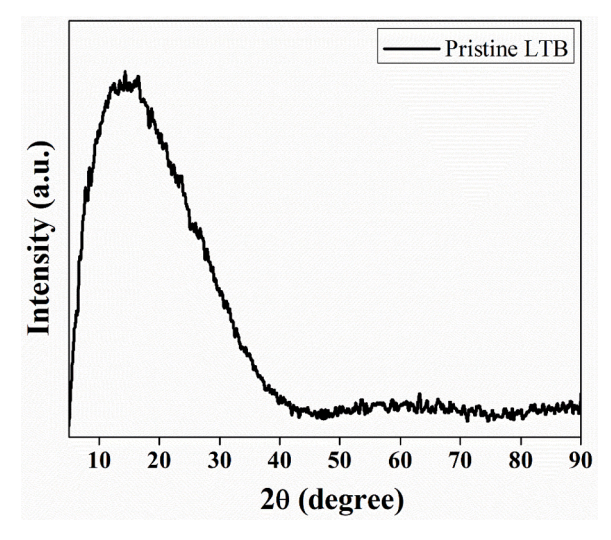


Fig. 3. The XRD pattern of pristine LTB glass.

Infrared spectrum (FTIR)

To understand the structural dynamics and fingerprints of structural units present in the glasses the FTIR spectra was recoded at room temperature from 400 cm⁻¹ to 4000 cm⁻¹. The bands between 400 cm⁻¹ to 1600 cm⁻¹ play a vital role in understanding the structure of LTB and vanadium doped LTB glasses. The glass composition shows six transmittance bands and they are assigned to various vibrational modes. The band at 464 cm $^{-1}$ corresponds to stretching (ν) oscillations of Te-O-Te bonds [34]. At 535 cm⁻¹ the band corresponds to vibrations of VO₂ groups of the VO₄ polyhedral unit due to addition of V₂O₅ in the glass matrix. The band present in the region 662 cm⁻¹ to 687 cm⁻¹ is due to bending (δ) vibration of B-O-B bonds. The band at 700 cm⁻¹ denotes bending (δ) oscillations of TeO₃/TeO₆ units due to the presence of tellurium in the prepared LTB glasses. The region 908 cm⁻¹ to 940 cm⁻¹ depicts symmetric stretching vibrations (ν_s) of B-O in BO₄ units and VO₂ group in VO₄ polyhedral unit. The band at 1200 cm⁻¹ to 1400 cm⁻¹ corresponds to ν_8 B-O in BO₃ unit of boroxol ring and BO₃ units in meta, pyroborate & orthoborate groups [35]. Fig. 4 and Table 3 shows the FTIR spectra of the glasses and its band assignment with corresponding patterns.

Raman spectra

Raman spectra was analysed for the powdered glass samples from $100~\rm cm^{-1}$ to $1500~\rm cm^{-1}$. The band from $421~\rm cm^{-1}$ to $463~\rm cm^{-1}$ corresponds to bending vibrations of Te-O -Te linkages [36]. The band at $610~\rm cm^{-1}$ is due to vibrations of TeO2 molecules and TeO4 units [37]. The band around 770 $\rm cm^{-1}$ to 780 $\rm cm^{-1}$ is due to presence of lithium ion in glass matrix [38]. As lithium concentration decreases, the intensity of the band decreases from LTB_0.5V to LTB_2V glasses. Symmetric stretching of V-O-V bonds in penta-coordinated VO4 groups are witnessed at 885 $\rm cm^{-1}$. The stretching modes of V^5+O4 tetrahedra with a V = O apex is seen from 900 $\rm cm^{-1}$ to 1050 $\rm cm^{-1}$ in vanadium doped LTB

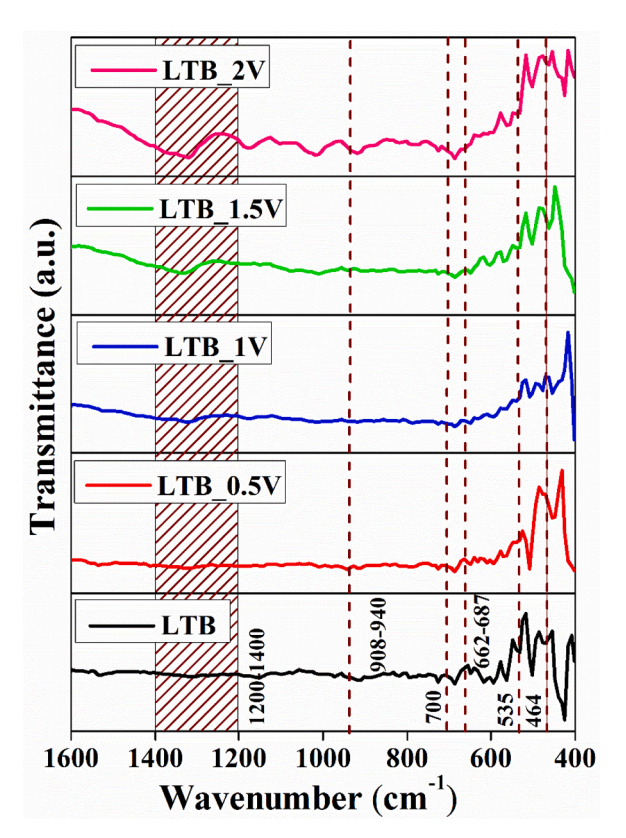


Fig. 4. The FTIR spectra of pristine and vanadium doped LTB glasses.

Table 3The peak position and band assignment for FTIR spectra of pristine and vanadium doped LTB glasses.

Wavenumber (cm ⁻¹)	Band assignment
464	ν oscillations of Te-O-Te bonds [34]
535	Vibrations of VO ₂ groups of the VO ₄ polyhedral unit [35]
662 - 687	δ B-O-B [34]
1200 - 1400	ν_s B-O in BO $_3$ unit of boroxol ring [35] ν_s of B-O in BO $_3$, units in meta, pyroborate & orthoborate
	groups [35]
700	δ oscillations of TeO ₃ /TeO ₆ units [34]
908–940	ν_s B-O stretching vibrations of tetrahedral BO ₄ units & VO ₂ group in VO ₄ polyhedral unit [34]

glasses and not in LTB glasses as it does not contain vanadium [39]. The region between 1250 $\rm cm^{-1}$ and 1500 $\rm cm^{-1}$ corresponds to stretching vibrations of B-O, BO₃-O-BO₄ and B-O-B bonds in BO₃ pyramidal units. The intensity of this band increases except for LTB_1.5V [37]. This may be due to the difference in the boron and oxygen bonds under the influence of vanadium. The Raman spectra of LTB and different concentrations of vanadium doped LTB are shown in Fig. 5 and the band assignments are given in Table 4.

Optical properties

UV-Visible spectroscopy

The optical absorption spectra were recorded for LTB to LTB_2V from 200 to 800 nm. The non- sharp absorption edges were observed proving the glassy nature of the samples. The direct bandgap (Eg) was calculated for the prepared glasses from Tauc's plot and is shown in Fig. 6. As vanadium concentration increases the Eg decreases from 2.74 eV to 2.16 eV [7]. The Urbach energy (Eu) measures the disorderliness of the material and depends on certain factors like temperature, thermal

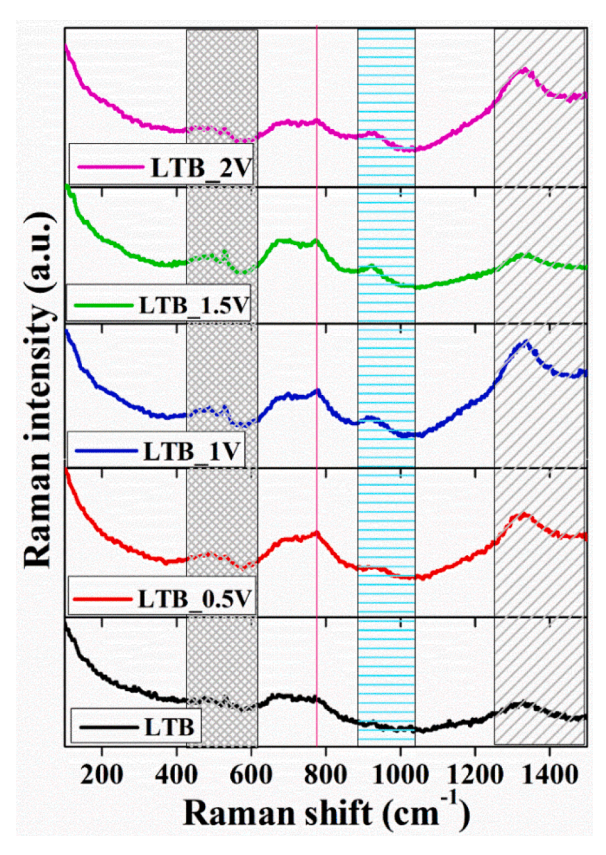
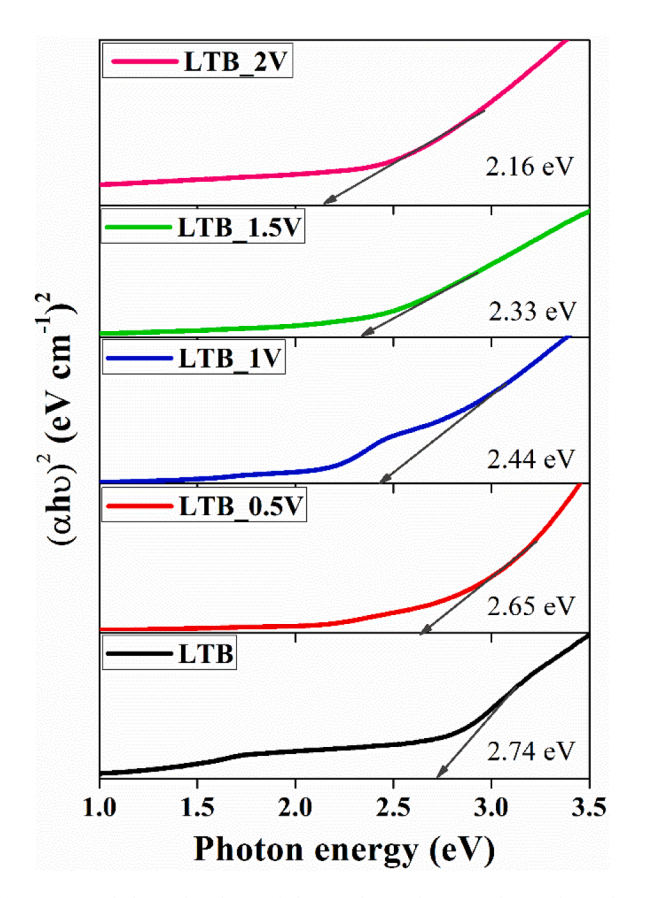


Fig. 5. The Raman spectra of LTB and vanadium doped LTB glasses.

Table 4The band assignment for Raman spectra of pristine and vanadium doped LTB glasses.

Pattern	Raman Shift (cm ⁻¹)	Band assignment
	421 - 463 610	Bending vibrations of Te-O -Te linkages [36] Vibrations of TeO ₂ molecules and TeO ₄ units [37]
	770 - 780	Presence of lithium oxide [38]
	885 900 - 1050	Symmetric stretching of V-O-V bonds in penta- coordinated VO ₄ groups [39] Stretching modes of $V^{5+}O_4$ tetrahedra with a $V=O$ apex [39]
	1250 - 1500	Stretching vibrations of B-O, BO $_3$ -O-BO $_4$ and B-O-B bonds in BO $_3$ pyramidal units [37]



 $\begin{tabular}{ll} \textbf{Fig. 6.} & \textbf{Optical direct bandgap of the synthesized LTB and vanadium doped LTB glasses.} \end{tabular}$

vibrations in the lattice, average photon energy, ionic bond and static disorder. The slope of the graph of ln (α) versus h ν gives E_u . Urbach energy is found to increase from 0.72 eV to 1.20 eV for increase in vanadium concentrations. The influence of vanadium has produced colour centres which leads to reduced optical transparency in LTB glasses. Pristine LTB glasses which is white turns to yellow and brown based on increasing concentration of vanadium. Larger the defect level energies, smaller the optical bandgap which allows electrons to move quickly from valence band to conduction band thereby increasing its conductivity [40]

Certain physical properties like refractive index (n), molar refractivity (R_m), reflection loss (L_r), transmission coefficient (T), molar polarizability (α_m) and metallization criteria (M) were determined from bandgap and is shown in Table 5.

Table 5Optical, electrical, and other physical parameters of LTB and vanadium doped LTB glasses

	LTB	LTB_0.5V	LTB_1V	LTB_1.5V	LTB_2V
Direct optical bandgap E_g (eV)	2.74	2.65	2.44	2.33	2.16
Urbach energy E_u (eV)	0.72	0.78	0.88	1.16	1.20
Refractive index n	2.47	2.49	2.56	2.60	2.66
Molar Refractivity R_m (cm ³ /mol)	27.97	27.48	27.34	26.88	26.59
Reflection loss L_r	0.18	0.18	0.19	0.20	0.20
Transmission coefficient <i>T</i>	0.69	0.69	0.68	0.67	0.66
Molar polarizability α_m (Å ³)	11.08	10.89	10.83	10.65	10.24
Metallization criteria M	0.37	0.36	0.35	0.34	0.33
Activation energy E_a (eV)	0.31	0.30	0.28	0.24	0.24

Physical properties

The refractive index (n) was estimated from bandgap using the Dimitrov Sakka relation [41],

$$\frac{n^2 - 1}{n^2 + 2} = 1 - \sqrt{\frac{E_g}{20}} \tag{1}$$

where, E_g is the optical bandgap. n is found to increase from 2.47 to 2.66 under the addition of vanadium which is due to creation of NBOs from breakage of glass networks which is in agreement with increase in density of the glass samples [42]. This increase in refractive index leads to a subsequent change in polarizability of the glasses. The decrease in bandgap with increase in refractive index and Urbach energy is shown in Fig. 7(a) and (b).

Using Lorentz - Lorentz formula, molar refractivity (R_m) and reflection loss (L_r) are given by the relation [42],

$$R_m = \frac{n^2 - 1}{n^2 + 2} \times V_m \tag{2}$$

$$L_r = \left(\frac{n-1}{n+1}\right)^2 \tag{3}$$

where, V_m is molar volume calculated from density.

Electronic polarizability (α_m) is the magnitude of electrons response to an applied magnetic field which is given by the following relation [41],

$$\alpha_m = \left(\frac{3}{4\pi N}\right) R_m \tag{4}$$

where, N is Avogadro's number. R_m depends on α_m of the material and is reported in Table 5. [43].

The transmission coefficient (T) is determined from the value of the refractive index by using the Fresnel's formula [43],

$$T = \frac{2n}{n^2 + 1} \tag{5}$$

The variation in the transmission coefficient with reflection loss again different concentration of vanadium in LTB glasses in show in Fig. 7(c) and Table 5. The transmission coefficient decreases from 0.6955 to 0.6569 as vanadium concentration increases this is due to the formation of colour centres that absorb light of specific wavelength and reducing the amount of light transmitted through the glass and increase the amount of light reflected. Therefore, the reflection loss is found to increase from 0.1795 to 0.2070 for increasing V_2O_5 content this is in agreement with telluroborate glass systems reported by Umar et. al [44]. Metallization criteria (M) based on refractive index is given by Eq. (6),

$$M = 1 - \frac{R_m}{V_m} \tag{6}$$

The metallization criteria decrease for the addition of vanadium from 0.37 to 0.33. The relation between OPD and M is shown in Fig. 7 (d). Oxide glasses with good nonlinearity have metallisation standard ranging from 0.35 to 0.45 as reported by Kh. S. Shaaban et. al. [45]. This

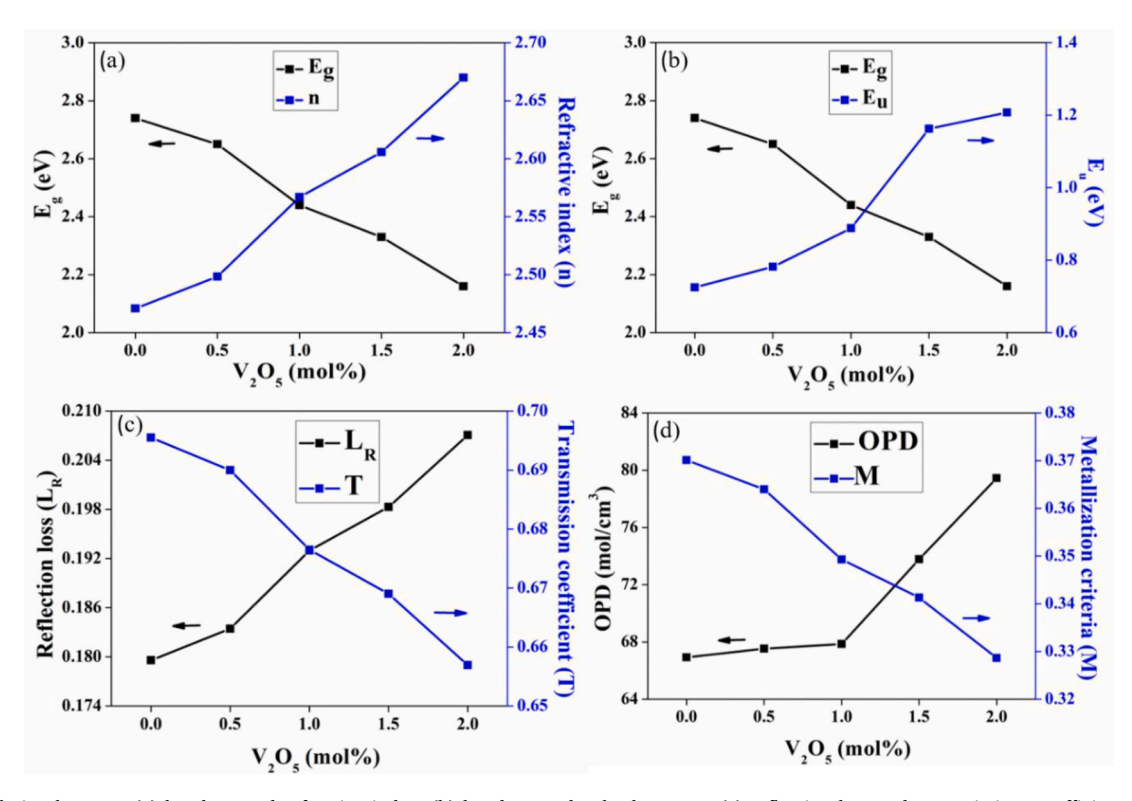


Fig. 7. The relation between (a) bandgap and refractive index, (b) bandgap and Urbach energy, (c) reflection loss and transmission co-efficient and (d) oxygen packing density and metallization criteria of the prepared LTB and vanadium doped LTB glasses.

confirms that LTB, LTB_0.5V and LTB_1V have good nonlinearity behaviour. Table 5 shows the variation in physical properties of the present LTB and vanadium doped LTB glass system.

Electrical properties

Dielectric constant

Dielectric constant (ϵ ') was calculated from the measured parallel capacitance of the electroded LTB glasses. The variation of dielectric constant as a function of temperature for various frequencies (100 kHz to 2000 kHz) is shown in Fig. 8. The dielectric constant increases with temperature and decreases with frequency. The higher values of ϵ ' at lower frequencies is due to interfacial polarisation i.e., charge accumulation at the interface (between electrodes and LTB glasses). These high values of ϵ ' at lower and medium frequencies makes LTB and vanadium doped LTB glasses suitable for optical devices [46]. The rise in ϵ ' with temperature is due to thermal activation of Li⁺, V⁴⁺ and V⁵⁺ ions.

The dielectric constant increases with addition of $\rm V_2O_5$ in the glass matrix and is maximum for LTB_1.5V. There is a slight decrease in the dielectric constant for higher concentration (LTB_2V). The dielectric loss was also measured for these glasses and it was found to decrease from nearly 0.25 for pristine to about 0.05 for all vanadium doped LTB glasses. The range of dielectric constant of vanadium and other transition metal doped borate glass systems and LTB_1.5V glass at 100 kHz is shown in Table 6. The LTB-1.5V glasses show good dielectric constant than other tabulated results [18,47,48]. The highest value of dielectric constant 19.07 was recorded for LTB_1.5V glasses.

A.C. conductivity

A.C conductivity (σ) was calculated from the conductance (G) measured using LCR meter [7]. Hopping mechanism and band conduction are responsible for electronic and ionic conduction in materials. High disordered shells provide suitable conditions for electron hopping in transition metal ions. The mobility of ions in the glass matrix increases

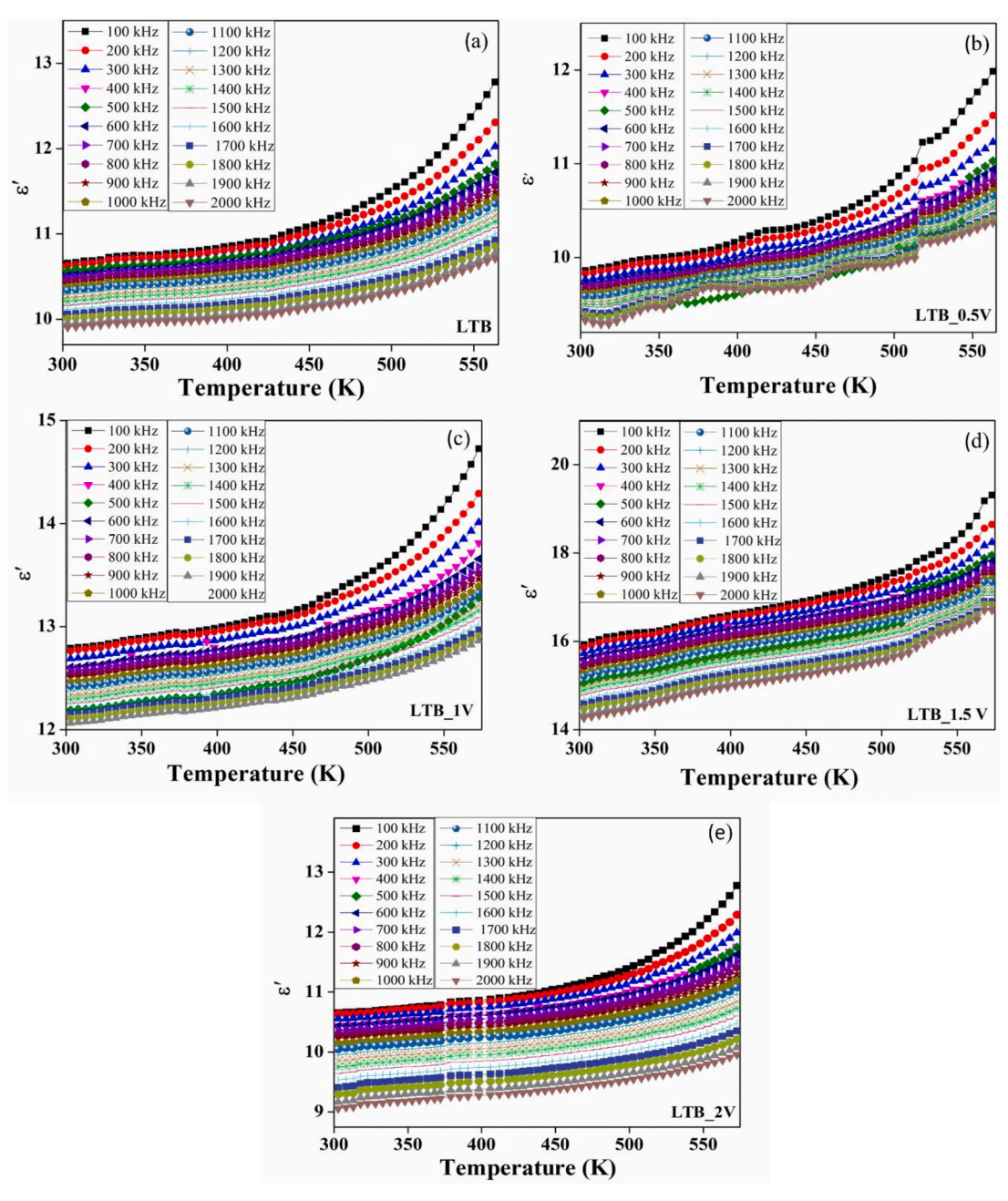


Fig. 8. Variation of dielectric constant at frequency ranging between 100 kHz to 2000 kHz from RT to 575 K.

Table 6
The dielectric constant of vanadium and other transition metal doped borate glass with LTB_1.5V glasses.

Glass networks	Glass composition	Dielectric constant
Vanadium doped lithium fluoride [18]	$0.25 \text{LiF} - 0.75 \text{B}_2 \text{O}_3 - 0.5 \text{V}_2 \text{O}_5$	17.05
Vanadium doped borate [47]	$15V_2O_5-85B_2O_3$	14.70
Copper doped sodium fluoroborate [48]	40 NaF-59B ₂ O ₃ -1CuO	13.98
Vanadium doped lithium telluroborate	$18.5 \text{Li}_2\text{O}\text{-}20 \text{TeO}_2\text{-}60 \text{B}_2\text{O}_3\text{-} \\ 1.5 \text{V}_2\text{O}_5$	19.07

with increase in temperature leading to increase in overall conductivity obeys Jonscher's universal power law [49]. The increase in electrical conductivity is due to both ionic and electronic conduction, where ionic conduction occurs due to immigration of Li⁺ ions and electronic

conduction occurs due to V⁴⁺ and V⁵⁺ (when local structural deformation takes place due to a phonon, an electron transforms by hopping from lower valance state to the higher valance state). Similarly, in the tellurium networks TeO₄ units are replaced with TeO₃ units thereby giving rise to electronic conductivity and is described by small polaron hopping (SPH) theory [50,51]. This is also accompanied by increase in the formation of NBOs in the glasses under the effect of vanadium and tellurium. Arrhenius plot of the prepared LTB glasses (ln σ versus 1000/T) was derived for frequencies 100 kHz to 400 kHz and is shown in Fig. 9. The activation energy of conduction at 100 kHz frequency was calculated and is shown in Fig. 10 (a). E_a decreases for increasing V_2O_5 concentrations from 0.3184 to 0.2473 eV and is given by Fig. 10 (b) and Table 5. The activation energy is lowest for LTB_1.5V glasses (0.2420 eV) thereby confirming its high electrical conductivity behaviour.

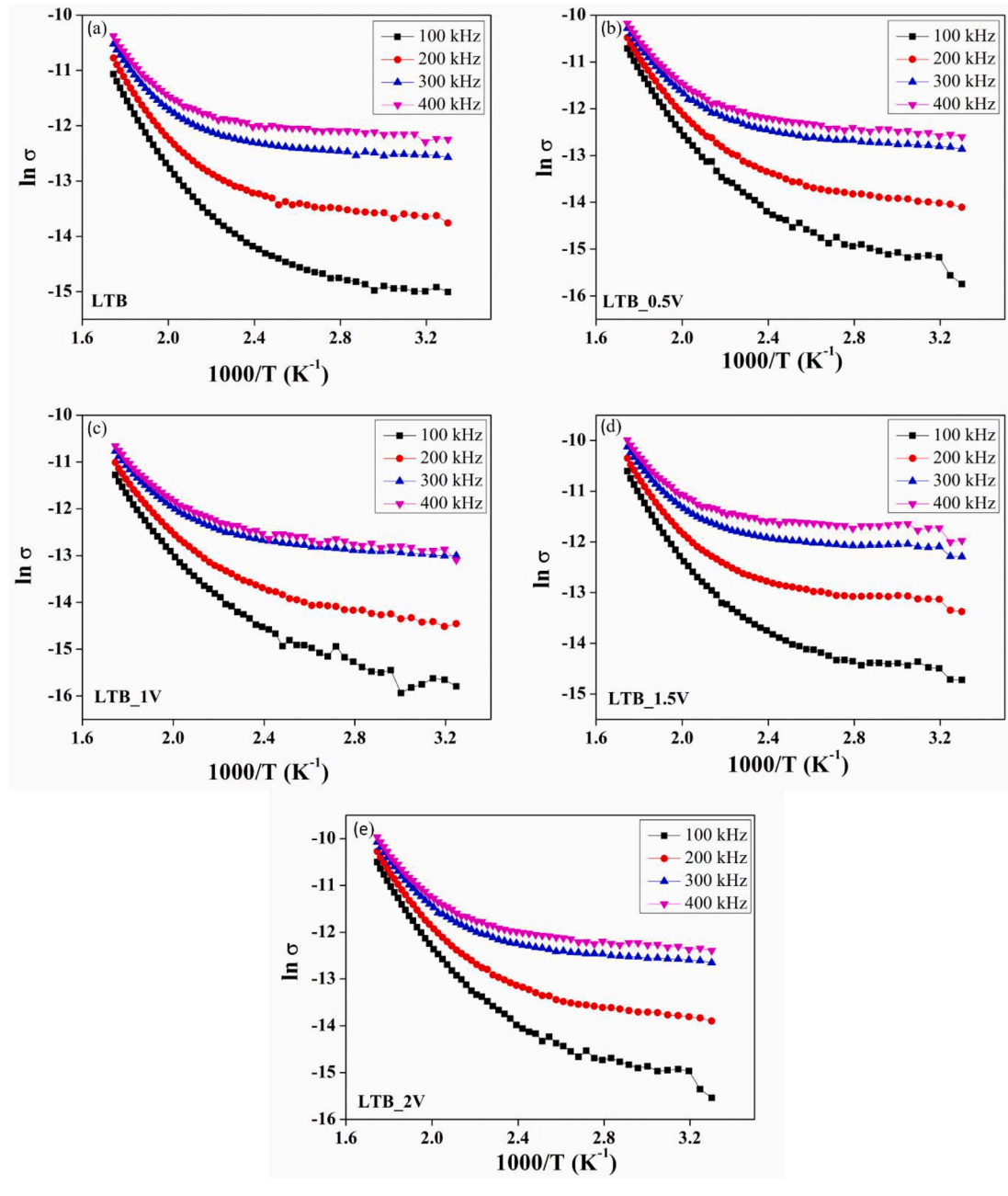


Fig. 9. Variation of ln σ at frequency ranging between 100 kHz to 400 kHz from RT to 575 K.

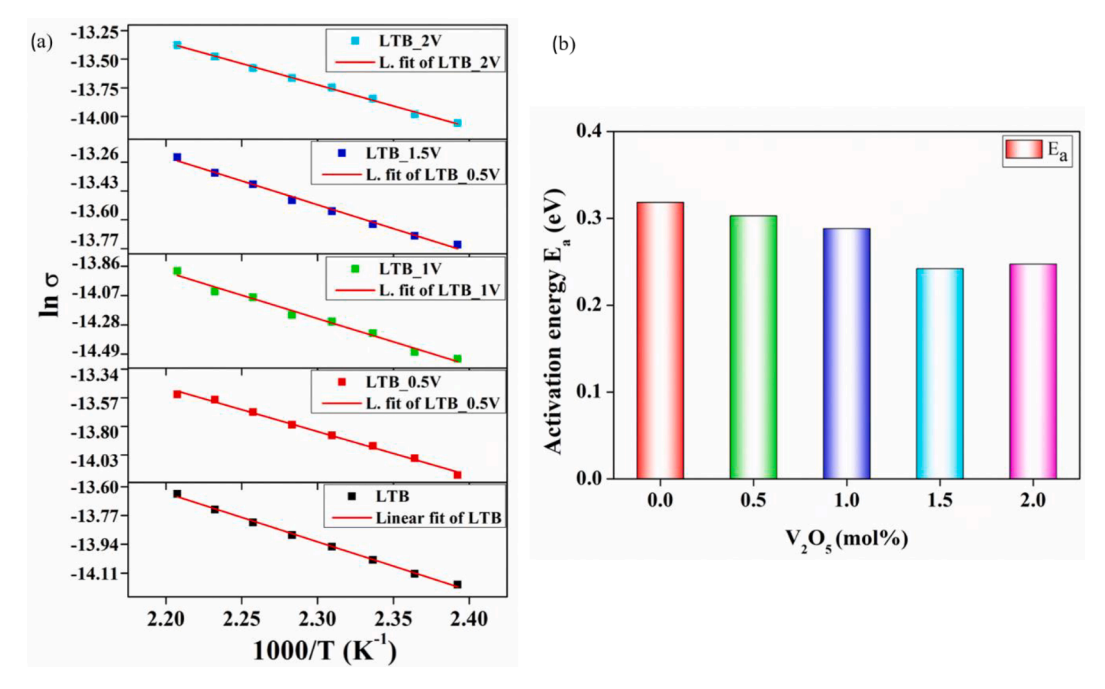


Fig. 10. (a) Linear fit of $\ln \sigma$ with temperature from RT to 575 K (b) Activation energy for all glasses at frequency of 100 kHz.

Radiation shielding

The prepared LTB glasses possess good efficiency to protect from gamma radiation due to the presence of TeO_2 which has high density of 5.67 g/cm³. The effect of vanadium in LTB and how it acts in radiation

shielding property is discussed below. Shielding parameters like mass attenuation coefficient (MAC), linear attenuation coefficient (LAC), half value layer (HVL), tenth value layer (TVL), mean free path (MFP), R value for Compton Scattering, atomic cross section (ACS), electronic cross section (ECS) from which effective electron density ($N_{\rm eff}$), effective

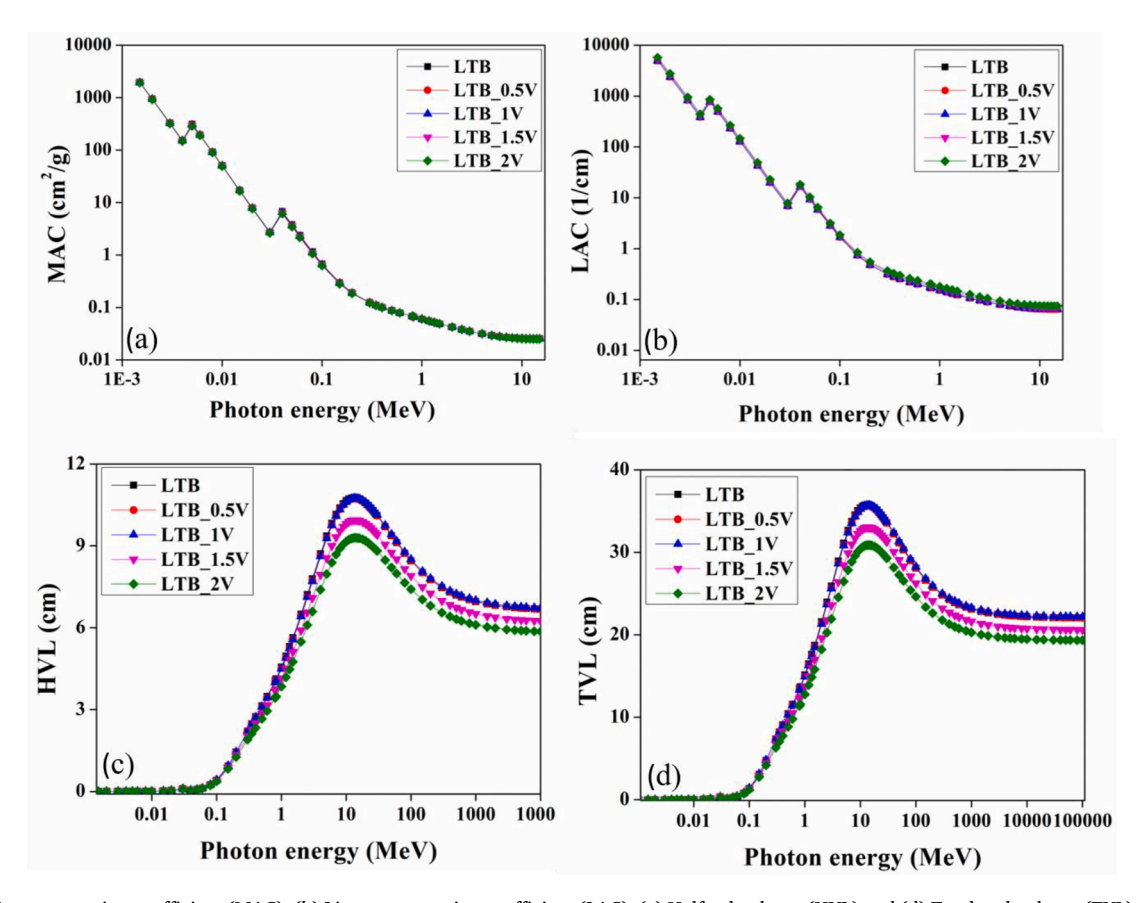


Fig. 11. (a) Mass attenuation coefficient (MAC), (b) Linear attenuation coefficient (LAC), (c) Half value layer (HVL) and (d) Tenth value layer (TVL) LTB and LTB_V glasses as a function of gamma energies

atomic number (Z_{eff}), and effective conductivity (C_{eff}) are studied to understand how vanadium doped LTB glasses supports in shielding.

MAC (μ_m) describes the interaction probability between gamma photons and the mass per unit are for certain medium. This is given by Beer-lambert law as follows [52],

$$I = I_o e^{-\mu t} \tag{7}$$

where, I and $\rm I_0$ are attenuated and un-attenuated photon intensities, μ is LAC and t is the thickness of the material [53]. The photon energy increases from 0.001 MeV to 15 MeV where the MAC and LAC decreases rapidly and then decreases gradually. For high photon energies the values of MAC and LAC remains unchanged and is shown in Fig. 11 (a) and (b). There are three factors responsible for decreasing LAC and MAC such as (i) Photoelectric effect (PE), (ii) Compton scattering (CS) and (iii) Pair production (PP) [54]. The rapid decline in MAC and LAC is due to photoelectric effect where maximum energy of photon is absorbed, the gradual decrease is due to Compton scattering and at very high energy (5–15 MeV) it denoted pair production.

The HVL and TVL are the thickness at which radiation intensities are reduced by one half and one tenth. There are determined from LAC by the following relation [52],

$$HVL = \frac{0.693}{\mu} \tag{8}$$

$$TVL = \frac{2.302}{\mu} \tag{9}$$

From the prepared LTB and vanadium doped LTB glasses, LTB_2V glasses which had maximum density has the least HVL and TVL proving it has best attenuation than the other glasses. LTB glasses of thickness $1.6~\rm mm$ can shield $0.015~\rm MeV$ of gamma rays whereas $1.4~\rm mm$ of LTB_2V can shielding the same energy. LTB_2V glasses has superior prospect of interactions with gamma photons leading to less transmission of these photons. The variation of HVL and TVL for different LTB glasses are shown in Fig. 11(c) and (d).

The MFP is the average distance between interaction of two gamma photons and is given by [55],

$$MFP = \frac{1}{\mu} \tag{10}$$

MFP is an important parameter to discuss the ability of any material to reduce gamma penetration. Lower the MFP, better the shielding ability i.e., good radiation absorbing material. On comparing the mean free path of LTB glasses series with already reported lithium borate glasses, the MFP of LTB glasses are lesser than lithium borate (LBO) glasses thereby proving its efficiency towards gamma ray shielding [7]. LTB_2V glasses possess lowest MFP than other glasses in this study and is shown in Fig. 12. At 3 MeV the mean free path decreases from 11.243 (LTB), 11.158 (LTB_0.5V), 11.116 (LTB_1V), 10.236 (LTB_1.5V) to 9.517 (LTB-2V). This confirms that LTB_2V has greater shielding properties among the other glasses that are considered in the present work. The inset of the Fig. 12 shows the difference in MFP of LTB_2V than other LTB glasses.

To see the effect of Compton scattering in the gamma ray absorption at a given energy range the R value is obtained using Eq. (11),

$$R = \frac{(\mu/\rho)_{cs}}{(\mu/\rho)_{tot}} \tag{11}$$

where, $(\mu/\rho)_{cs}$ is MAC of Compton scattering $(\mu/\rho)_{tot}$ MAC of total scattering. R value obtained is almost unity and is shown in Fig. 13 (a). This denoted that all contribution to LAC is due to CS. The ACS and ECS are found to decrease sharply till 0.01 MeV as in shown in Fig. 13 (b) and (c). The N_{eff} and Z_{eff} are calculated from ACS and ECS.

The effective electron density (N_{eff}) and effective atomic number (Z_{eff}) are important parameter for radiation shielding materials and is

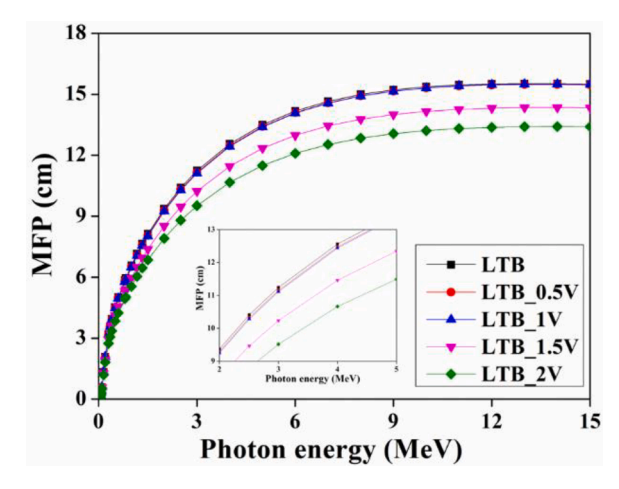


Fig. 12. The mean free path (MFP) of prepared glasses and inset: close view of MFP as a function of gamma energies

expressed by the following relations [1,56],

$$N_{eff} = \frac{MAC}{\sigma_{el}} \tag{12}$$

$$Z_{eff} = \frac{\sigma_a}{\sigma_{el}} \tag{13}$$

where, σ_a and σ_{el} are the total atomic cross section (ACS) and total electronic cross section (ECS) respectively. There is an increase in N_{eff} and Z_{eff} below 0.1 MeV and decreases after that which is due to domination of pair production in the energy region. Z_{eff} is maximum at 0.04 MeV for all the LTB glasses. It is found to decrease from 45.03 (LTB), 44.75 (LTB_0.5V), 44.47 (LTB_1V), 44.17 (LTB_1.5V) and 43.87 (LTB_2V). The effective conductivity (C_{eff}) also shows similar trend as N_{eff} and Z_{eff} and is shown in Fig. 14. C_{eff} corresponds to number of free electrons resulting from photon matter interaction (PE, CS and PP) and is directly proportional to N_{eff} , Z_{eff} and densities of materials [57]. Therefore, the presence of TeO_2 and incorporation of V_2O_5 content in LTB glasses raised the shielding competency against gamma photons.

Conclusion

The influence of V₂O₅ addition on the structural, optical, physical, electrical and radiation shielding properties of lithium telluro-borate glass has been investigated. Density of the glasses were found to increase from 2.52 to $2.98~g/cm^3$ under addition of V_2O_5 from which certain structural parameters like V_m , V_o , OPD, $d_{B\text{-}B_1}$, n_b , Λ_{th} , I_c , C_c and μ_{cal} were determined. XRD pattern confirms the amorphous nature of LTB glass. The presence of tellurium, vanadium, and lithium bonds along with their functional groups in the borate glass matrix was confirmed from FTIR and Raman spectroscopic investigations. The optical bandgap was found to decrease with increase in Urbach energy for increasing vanadium concentration in LTB glasses. Physical parameters like n, R_m , L_r , T, α_m and M were analysed. The dielectric constant and A. C. conductivity of the samples were found to increase under the influence of vanadium and activation energy was decreasing. LTB_1.5V shows the least activation energy. The conduction mechanism was due to ionic and electronic conduction from Li $^{\!+},\,V^{4+},\,V^{5+}$ and tellurium ions on bases of small polaron hopping theory. Radiation attenuation behaviour of LTB and vanadium doped LBT glasses were studied using Phy-X/PSD software for gamma energies ranging from 0.001 MeV to 15 MeV. LTB_2V glasses was found to exhibit greater shielding ability than other LTB glasses.

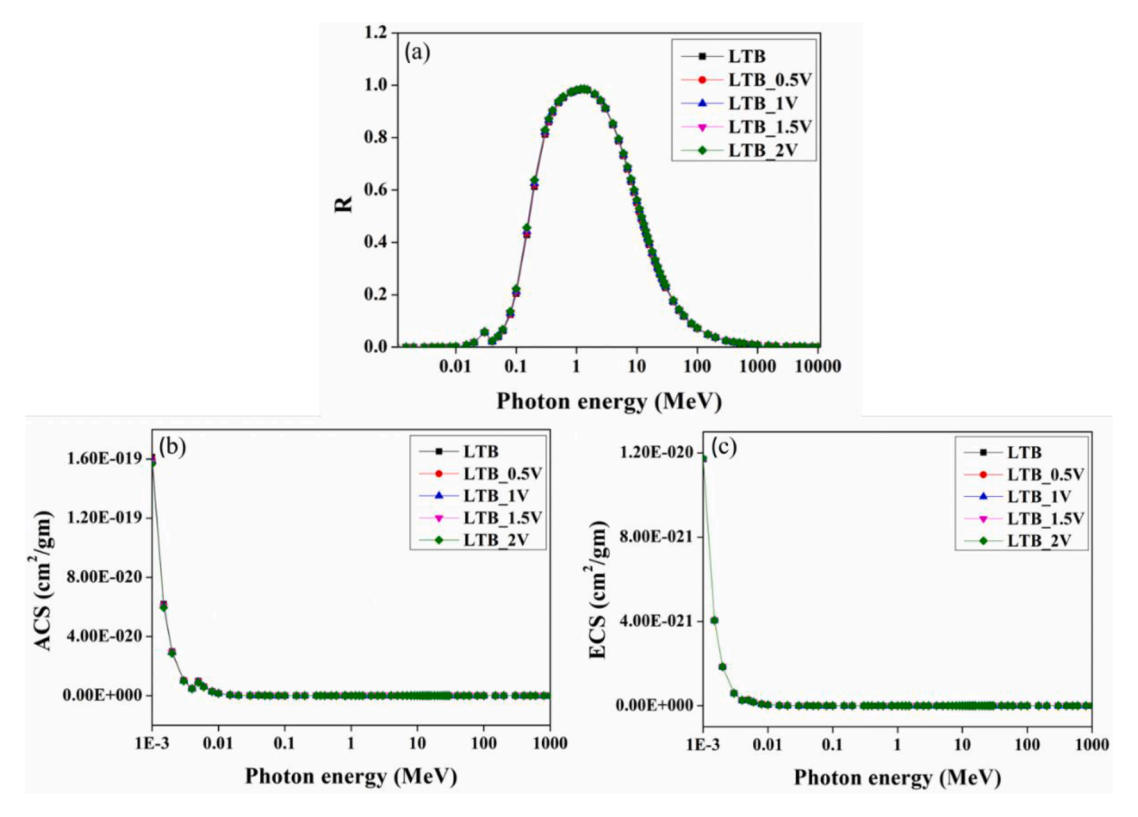


Fig. 13. (a) R (b) atomic cross section (ACS) and (c) electronic cross section (ECS) of LTB and LTB_V glasses as a function of gamma energies

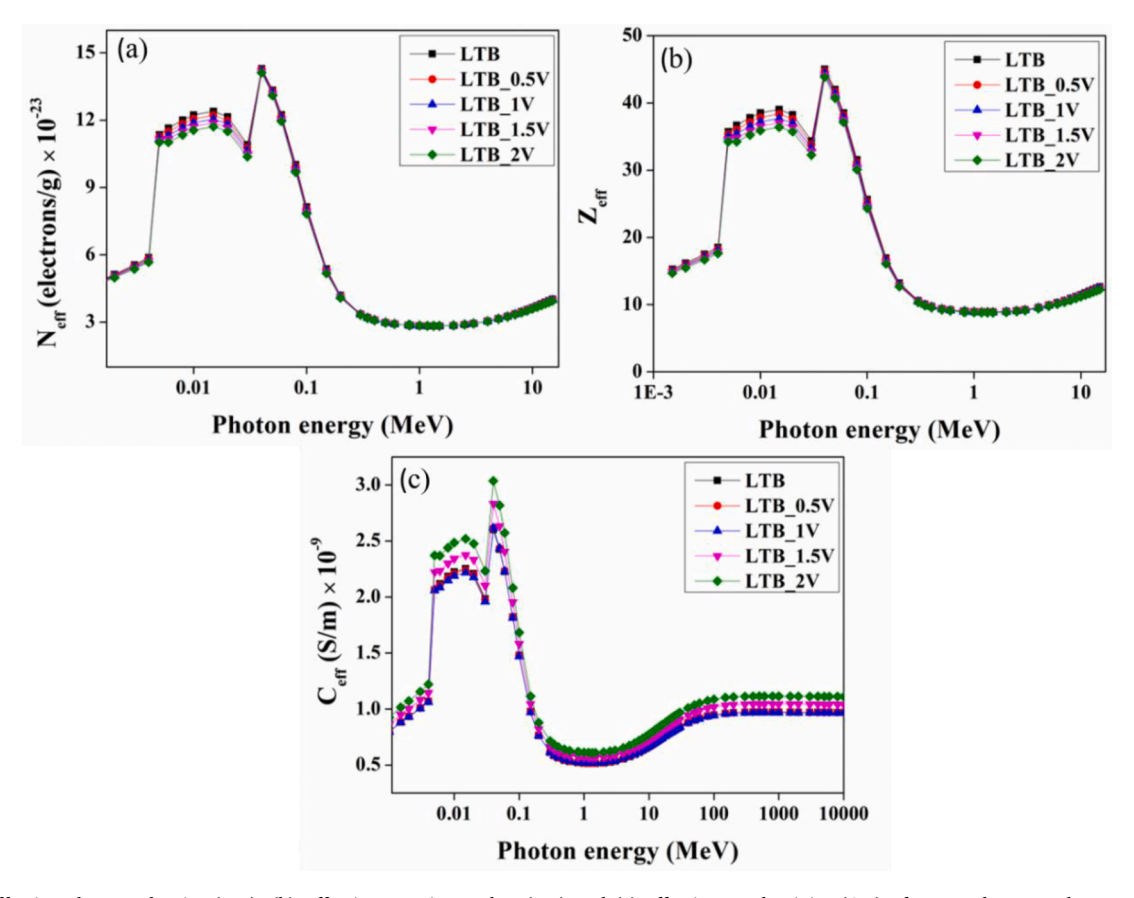


Fig. 14. (a) Effective electron density ($N_{\rm eff}$), (b) Effective atomic number ($Z_{\rm eff}$) and (c) effective conductivity ($C_{\rm eff}$) of LTB and LTB_V glasses as a function of gamma energies.

Research data

Research data will be made available on request to authors.

CRediT authorship contribution statement

S Karthika: Conceptualization, Investigation, Validation, Writing – original draft, Methodology, Resources, Formal analysis. S Shanmuga Sundari: Investigation, Validation, Writing – review & editing, Funding acquisition. K Marimuthu: Methodology, Writing – review & editing. P Meena: Validation, Writing – review & editing.

Declaration of Competing Interest

The authors declare that they have no known competing financial interests or personal relationships that could have appeared to influence the work reported in this paper.

Data availability

Data will be made available on request.

Acknowledgment

Authors SK and SSS acknowledge the financially support provided by UGC, New Delhi in the form of User Funded Research project UFR No. [66306].

References

- M. Rashad, A.M. Ali, M.I. Sayyed, H.H. Somaily, H. Algarni, Y.S. Rammah, Radiation attenuation and optical features of lithium borate glasses containing barium: B₂O₃.Li₂O.BaO, Ceram. Int. 46 (2020) 21000, https://doi.org/10.1016/j. ceramint.2020.05.165.
- [2] M. Muradov, M.B. Baghirov, G. Eyvazova, L. Gahramanli, S. Mammadyarova, G. Aliyeva, E. Huseynov, M. Abdullayev, Influence of gamma radiation on structure, morphology, and optical properties of GO and GO/PVA nanocomposite, Radiat. Phys. Chem. 208 (2023), 110926, https://doi.org/10.1016/j. radphyschem.2023.110926.
- [3] K. Fujimoto, J.A. Wilson, J.P. Ashmore, Radiation exposure risks to nuclear well loggers, Health Phys. 48 (1985) 437, https://doi.org/10.1097/00004032-198504000-00006.
- [4] W. Guo-hui, H. Man-li, C. Fan-chao, F. Jun-dong, D. Yao-dong, Enhancement of flame retardancy and radiation shielding properties of ethylene vinyl acetate-based radiation shielding composites by EB irradiation, Prog. Nucl. Energy 112 (2019) 225, https://doi.org/10.1016/j.pnucene.2019.01.001.
- [5] T. Shams, M. Eftekhar, A. Shirani, Investigation of gamma radiation attenuation in heavy concrete shields containing hematite and barite aggregates in multi-layered and mixed forms, Constr. Build. Mater. 182 (2018) 35, https://doi.org/10.1016/j. conbuildmat.2018.06.032.
- [6] M. Kurudirek, Heavy metal borate glasses: potential use for radiation shielding, J. Alloys Compd. 727 (2017) 1227, https://doi.org/10.1016/j. iallcom.2017.08.237.
- [7] S. Karthika, K. Marimuthu, R.C. Meena, I. Sulania, K. Asokan, S. Shanmuga Sundari, Gamma irradiation-induced changes in the structural, optical, electrical and radiation shielding properties of lithium borate glasses, Radiat. Phys. Chem. 202 (2023), 110560, https://doi.org/10.1016/j.radphyschem.2022.110560.
- [8] S. Karthika, K. Asokan, K. Marimuthu, P.E. Teresa, R.C. Meena, A. Durairajan, M. A. Valente, P. Meena, S. Shanmuga Sundari, Structural and optical properties of lithium borate glasses under extreme conditions of ion irradiation, Phys. Scr. 98 (2023), https://doi.org/10.1088/1402-4896/ace139.
- [9] A. Abdelghany, H.A. Elbatal, L. Marei, Optical and shielding behavior studies of vanadium-doped lead borate glasses, Radiat. Eff. Defects Solids 167 (1) (2011), https://doi.org/10.1080/10420150.2011.629418.
- [10] N.S. Sabri, A.K. Yahya, R. Abd-Shukor, M.K. Talari, Anomalous elastic behaviour of xSrO-10PbO-(90-x)B₂O₃ glass system, J. NonCryst. Solids 444 (2016) 55, https://doi.org/10.1016/j.inoncrysol.2016.04.038.
- [11] R. El-Mallawany, F.I. El-Agawany, M.S. Al-Buriahi, C. Muthuwong, A. Novatski, Y. S. Rammah, Optical properties and nuclear radiation shielding capacity of TeO₂-Li₂O-ZnO glasses, Opt. Mater. 106 (2020), 109988, https://doi.org/10.1016/j.optmat.2020.109988
- [12] M.I. Sayyed, et al., Effect of TeO₂ addition on the gamma radiation shielding competence and mechanical properties of boro-tellurite glass: an experimental approach, J. Mater. Res. Technol. 18 (2022) 1017, https://doi.org/10.1016/j.jmrt.2022.02.130.

- [13] S. Kabi, A. Ghosh, Mixed glass former effect in AgI doped silver borophosphate glasses, Solid State Ion. 262 (2014) 778, https://doi.org/10.1016/j. ssi 2013.09.028
- [14] O. Ravi, C.M. Reddy, B.S. Reddy, B.Deva Prasad Raju, Judd–Ofelt analysis and spectral properties of Dy³⁺ ions doped niobium containing tellurium calcium zinc borate glasses, Opt. Commun. 312 (2014) 263, https://doi.org/10.1016/j. optcom.2013.09,044.
- [15] C. Nelson, T. Furukawa, W.B. White, Transition metal ions in glasses: network modifiers or quasi-molecular complexes? Mater. Res. Bull. 18 (1983) 959, https://doi.org/10.1016/0025-5408(83)90007-7.
- [16] K. Siva Rama Krishna Reddy, K. Swapna, S.K. Mahamuda, M. Venkateswarlu, M.V. V.K. Srinivas Prasad, A.S. Rao, G. Vijaya Prakash, Structural, optical absorption and photoluminescence spectral studies of Sm³⁺ ions in Alkaline-Earth Boro Tellurite glasses, Opt. Mater. 79 (2018) 21, https://doi.org/10.1016/j.optmat.2018.03.005.
- [17] S. Khan, K. Singh, Structural, optical, thermal and conducting properties of V_2 -xLixO₅- δ (0.15 \leq x \leq 0.30) systems, Sci. Rep. 10 (2020) 1089, https://doi.org/10.1038/s41598-020-57836-8.
- [18] A.M. Abdel-karim, A.M. Fayad, I.M. El-kashef, H.A. Saleh, Influence of vanadium oxide on the optical and electrical properties of Li (Oxide or Fluoride) borate glasses, J. Electron. Mater. 52 (2023) 2409, https://doi.org/10.1007/s11664-022-10187-8.
- [19] O. Chukova, S. Nedilko, V. Scherbatskyi, Development of borate-vanadate glass pure and incorporated with La-vanadate nanoparticles, Acta Phys. Pol. A 141 (2022) 345, https://doi.org/10.12693/APhysPolA.141.345.
- [20] K. Kaur, K.J. Singh, V. Anand, Structural properties of Bi₂O₃–B₂O₃–SiO₂–Na₂O glasses for gamma ray shielding applications, Radiat. Phys. Chem. 120 (6) (2016), https://doi.org/10.1016/j.radphyschem.2015.12.003.
- [21] S.A.M. Issa, A. Kumar, M.I. Sayyed, M.G. Dong, Y. Elmahroug, Mechanical and gamma-ray shielding properties of TeO₂-ZnO-NiO glasses, Mater. Chem. Phys. 212 (2018) 12, https://doi.org/10.1016/j.matchemphys.2018.01.058.
- [22] H.O. Tekin, S.A.M. Issa, E. Kavaz, E.E. Altunsoy Guclu, The direct effect of Er₂O₃ on bismuth barium telluro borate glasses for nuclear security applications, Mater. Res. Express (6) (2019), 115212, https://doi.org/10.1088/2053-1591/ab4cb5.
- [23] Y.S. Rammah, E. Kavaz, H. Akyildirim, F.I. El-Agawany, Evaluation of photon, neutron, and charged particle shielding competences of TeO₂-B₂O₃-Bi₂O₃-TiO₂ glasses, J. NonCryst. Solids 535 (2020), 119960, https://doi.org/10.1016/j. jnoncrysol.2020.119960.
- [24] Y. Al-Hadeethi, M.I. Sayyed, A comprehensive study on the effect of TeO₂ on the radiation shielding properties of TeO₂–B₂O₃–Bi₂O₃–LiF–SrCl₂ glass system using Phy-X /PSD software, Ceram. Int. 46 (2020) 6136, https://doi.org/10.1016/j. ceramint.2019.11.078.
- [25] R. Kaur, R. Kaur, A. Khanna, F. González, Structural and thermal properties of vanadium tellurite glasses, AIP Conf. Proc. 1942 (2018), 070028, https://doi.org/ 10.1063/1.5028826.
- [26] M.H.M. Zaid, K.A. Matori, H.A.A. Sidek, I.R. Ibrahim, Bismuth modified gamma radiation shielding properties of titanium vanadium sodium tellurite glasses as a potent transparent radiation-resistant glass applications, Nucl. Eng. Technol. 53 (2021) 1323. https://doi.org/10.1016/j.net.2020.10.006.
- (2021) 1323, https://doi.org/10.1016/j.net.2020.10.006.
 [27] H.A. Thabit, A.K. Ismail, H.E. Soufi, D.A. Abdulmalik, A.M. Al-Fakih, S. Alraddadi, M.I. Sayyed, Structural, thermal, and mechanical investigation of telluro-borate-Bismuth glass for radiation shielding, J. Mater. Res. Technol. 24 (2023) 4353, https://doi.org/10.1016/j.jmrt.2023.04.082.
- [28] I. Mechrgui, A. Ben Gouider Trabelsi, F.H. Alkallas, S. Nasri, H. Elhouichet, Mixed ionic and electronic conduction in TeO₂-ZnO-V₂O₅ glasses towards good dielectric features, Materials 21 (2022), https://doi.org/10.3390/ma15217659, 15.
- [29] L. McDonald, C. Siligardi, M. Vacchi, A. Zieser, M. Affatigato, Tellurium vanadate glasses: V⁴⁺ colorimetric measure and its effect on conductivity, Front. Mater. Orig. Res. 7 (103) (2020), https://doi.org/10.3389/fmats.2020.00103.
- [30] S. Dalal, S. Khasa, M.S. Dahiya, A. Yadav, A. Agarwal, S. Dahiya, Optical and thermal investigations on vanadyl doped zinc lithium borate glasses, J. Asian Ceram. Soc. 3 (2015) 234, https://doi.org/10.1016/j.jascer.2015.03.004.
- [31] Y. Yang, I.D. Sommerville, A. McLean, Some fundamental considerations pertaining to oxide melt interactions and their influence on steel quality, Trans. Indian Inst. Met. 59 (2006) 655.
- [32] R. Divina, K.A. Naseer, K. Marimuthu, Y.S.M. Alajerami, M.S. Al-Buriahi, Effect of different modifier oxides on the synthesis, structural, optical, and gamma/beta shielding properties of bismuth lead borate glasses doped with europium, J. Mater. Sci. Mater. Electron. 31 (2020) 21486, https://doi.org/10.1007/s10854-020-04662-3.
- [33] K. Annapoorani, K. Marimuthu, Spectroscopic properties of Eu³⁺ ions doped Barium telluroborate glasses for red laser applications, J. NonCryst. Solids 463 (2017) 148, https://doi.org/10.1016/j.jnoncrysol.2017.03.004.
- [34] R.L.D. Virender Kundu, A.S. Maan, D.R. Goyal, S. Arora, Characterization and electrical conductivity of Vanadium doped strontium bismuth borate glasses, J. Optoelectron. Adv. Mater. 12 (2010) 2373.
- [35] E. Ilik, G. Kilic, U.G. Issever, Synthesis of novel AgO-doped vanadium-borophosphate semiconducting glasses and investigation of their optical, structural, and thermal properties, J. Mater. Sci. Mater. Electron. 31 (11) (2020) 8986, https://doi.org/10.1007/s10854-020-03432-5.
- [36] C.H.B. Annapurna Devi, S. Mahamuda, K. Swapna, M. Venkateswarlu, A. Srinivasa Rao, G. Vijaya Prakash, Compositional dependence of red luminescence from Eu³⁺ ions doped single and mixed alkali fluoro tungsten tellurite glasses, Opt. Mater. 73 (2017) 260, https://doi.org/10.1016/j.optmat.2017.08.010.

- [37] F. He, Z. He, J. Xie, Y. Li, IR and Raman Spectra Properties of Bi₂O₃-ZnO-B₂O₃-BaO Quaternary Glass System, Am. J. Anal. Chem. 05 (2014) 1142, https://doi.org/ 10.4236/ajac.2014.516121.
- [38] A. Osipov, L. Osipova, Structure of lithium borate glasses and melts: Investigation by high temperature Raman spectroscopy, Phys. Chem. Glas. Eur. J. Glass Sci. Technol. B 50 (2009) 343.
- [39] M.R. Cicconi, Z. Lu, T. Uesbeck, L. van Wüllen, D.S. Brauer, D. De Ligny, Influence of vanadium on optical and mechanical properties of aluminosilicate glasses, Front. Mater. Orig. Res. 7 (2020), https://doi.org/10.3389/fmats.2020.00161.
- [40] N. Zaini, S. Mohamed, Z. Mohamed, Effect of vanadium on structural and optical properties of borate glasses containing Er³⁺ and silver nanoparticles, Materials 14 (2021) 3710, https://doi.org/10.3390/ma14133710.
- [41] M.K. Halimah, M.F. Faznny, M.N. Azlan, H.A.A. Sidek, Optical basicity and electronic polarizability of zinc borotellurite glass doped La³⁺ ions, Results Phys. 7 (2017) 581, https://doi.org/10.1016/j.rinp.2017.01.014.
- [42] H.K. Obayes, H. Wagiran, R. Hussin, M.A. Saeed, Structural and optical properties of strontium/copper co-doped lithium borate glass system, Mater. Des. 94 (2016) 121, https://doi.org/10.1016/j.matdes.2016.01.018.
- [43] A.A. Ali, Y.S. Rammah, M.H. Shaaban, The influence of TiO₂ on structural, physical and optical properties of B₂O₃·TeO₂-Na₂O-CaO glasses, J. NonCryst. Solids 514 (2019) 52, https://doi.org/10.1016/j.jnoncrysol.2019.03.030.
- [44] S.N. Nazrin, S.A. Umar, M.K. Halimah, M.M. Marian, Z.W. Najwa, M.S. Jufa, M. T. Syahirah, Z. Zuhasanah, M.N. Azlan, I.G. Geidam, I. Boukhris, I. Kebaili, Dielectric constant, metallization criterion and optical properties of CuO doped TeO₂–B₂O₃ glasses, J. Inorg. Organomet. Polym. Mater. 32 (2022) 2513, https://doi.org/10.1007/s10904-022-02244-w.
- [45] K.S. Shaaban, E.S. Yousef, Optical properties of Bi₂O₃ doped boro tellurite glasses and glass ceramics, Optik 203 (2020), 163976, https://doi.org/10.1016/j. iileo 2019 163976
- [46] I. Mechergui, A. trabelsi, F. Alkallas, s. nasri, H. Elhouichet, Mixed ionic and electronic conduction in TeO₂-ZnO-V₂O₅ glasses towards good dielectric features, Materials 15 (2022) 7659, https://doi.org/10.3390/ma15217659.

- [47] R. Amnerkar, C. Adgaonkar, S. Yawale, S. Yawale, Microwave properties of vanadium borate glasses, Bull. Mater. Sci. 25 (2002) 431, https://doi.org/ 10.1007/BE02708022
- [48] M.K. Murthy, K.S.N. Murthy, N. Veeraiah, Dielectric properties of NaF-B₂O₃ glasses doped with certain transition metal ions, Bull. Mater. Sci. 23 (2000) 285, https:// doi.org/10.1007/BF02720084.
- [49] S.S. Sankaran, B. Kumar, A. Kandasami, R. Dhanasekaran, Effect of SHI irradiation on NBT–BT ceramics: transformation of relaxor ferroelectric to ferroelectric nature, Appl. Surf. Sci. 265 (2013) 296, https://doi.org/10.1016/j.apsusc.2012.10.199.
- [50] S. Khan, K. Singh, Structural, optical, thermal and conducting properties of V_2 -xLixO₅- δ (0.15 \leq x \leq 0.30) systems, Sci. Rep. 10 (2020) 1089, https://doi.org/10.1038/s41598-020-57836-8.
- [51] D. Souri, P. Azizpour, H. Zaliani, Electrical conductivity of V₂O₅-TeO₂-Sb glasses at low temperatures, J. Electron. Mater. 43 (2014) 3672, https://doi.org/10.1007/ s11664-014-3288-x.
- [52] E. Sakar, P.X. Team, B. Alım, M. Kurudirek, Phy-X /PSD: development of a user-friendly online software for calculation of parameters relevant to radiation shielding and dosimetry, Radiat. Phys. Chem. 166 (2019), https://doi.org/10.1016/j.radphyschem.2019.108496.
- [53] G. Singh, et al., Analysis of enhancement in Gamma ray shielding proficiency by adding WO₃ in Al₂O₃-PbO-B₂O₃ glasses using Phy-X/PSD, J. Mater. Res. Technol. 9 (2020) 14425, https://doi.org/10.1016/j.jmrt.2020.10.020.
- [54] S.A.M. Issa, M.I. Sayyed, M. Kurudirek, Study of gamma radiation shielding properties of ZnO-TeO glasses, Bull. Mater. Sci. 40 (2017) 841, https://doi.org/ 10.1007/s12034-017-1425-x.
- [55] Y. Alhadeethi, Radiation attenuation properties of Bi₂O₃–Na₂O–V₂O₅–TiO₂–TeO₂ glass system using Phy-X /PSD software, Ceram. Int. 46 (4) (2020), https://doi.org/10.1016/j.ceramint.2019.10.212.
- [56] Y.Y. Celen, I. Akkurt, H.F. Kayıran, Gamma ray shielding parameters of barium tetra titanate (BaTi₄O₉) ceramic, J. Mater. Sci. Mater. Electron. 32 (2021) 18351, https://doi.org/10.1007/s10854-021-06376-6.
- [57] Z. Aygun, M. Aygun, Radiation shielding potentials of rene alloys by Phy-X/PSD code, Acta Phys. Pol. A 141 (2022) 507, https://doi.org/10.12693/APhysPolA.141.507.